

# AePW-3

# High Speed Working Group

## RC-19 Wind Tunnel

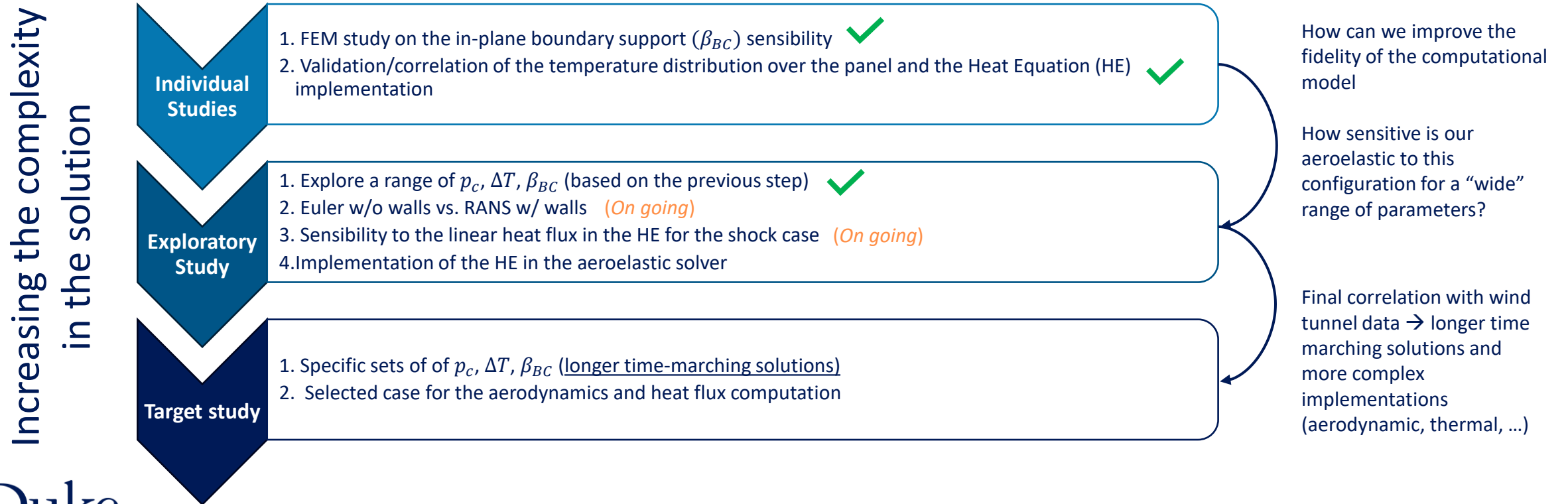
2024 Updates

Aeroelasticity Laboratory | Duke University

Luisa Piccolo Serafim, Earl Dowell

# Motivation For Our Work

- To provide the highest possible fidelity in the computational model at an affordable cost; orders of magnitude reduction in cost compared to traditional CFD/CSD methods
- To explore a wide range of relevant parameters including  $M_\infty$ ,  $Re$ , static pressure differential, thermal stresses and structural boundary conditions, both out of plane and in plane.
- To correlate computational results with experimental results and assess the sensitivity of these results to uncertainties in key parameters



# Computational Method

## Nonlinear Aeroelastic Model

$$\underbrace{M_{m,n}\ddot{q}_n(t) + C_{m,n}\dot{q}_n(t) + G_{m,n}^{(2)}q_n(t)}_{\text{Linear plate model}} + \underbrace{D_{m,n,r,p}^{(2)}q_n(t)q_r(t)q_p(t)}_{\text{NL structural stiffness}} + \underbrace{Q_{m,n}^{Aero}}_{\text{Aero}} = 0$$

$$\underbrace{L_{n,m}^c P_n(t)}_{\text{Cavity coupling}} + \underbrace{Q_m^{static}}_{\text{Static pressure differential}} = 0$$

Static pressure differential sensitivity ( $\Delta p = p_\infty - p_c$ )

In-plane Boundary sensitivity + Thermal Buckling ( $\Delta T$ )

Acoustic Modes don't play a significant effect in the panel dynamic response (for the RC-19 model)

### Unsteady Aerodynamics Model

- Linear Piston Theory
- Full Potential Aerodynamics
- Dynamically Linearized Time-domain Approach
  - Euler
  - Navier-Stokes (RANS)

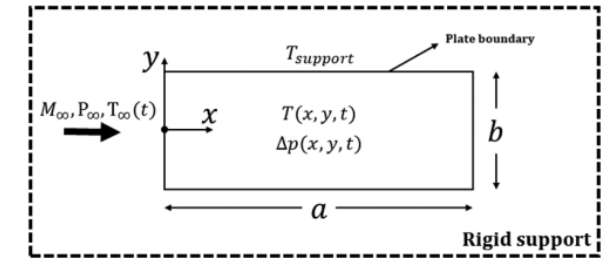


Fig. 1 Plate top view with freestream flow, static pressure differential, and support and plate temperatures.

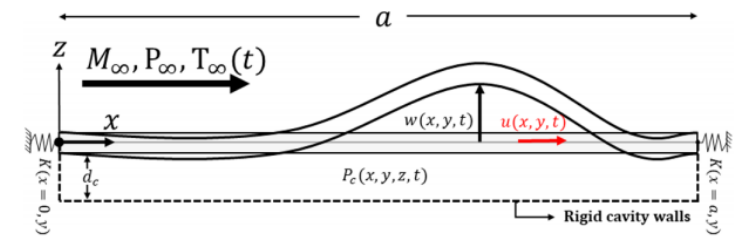
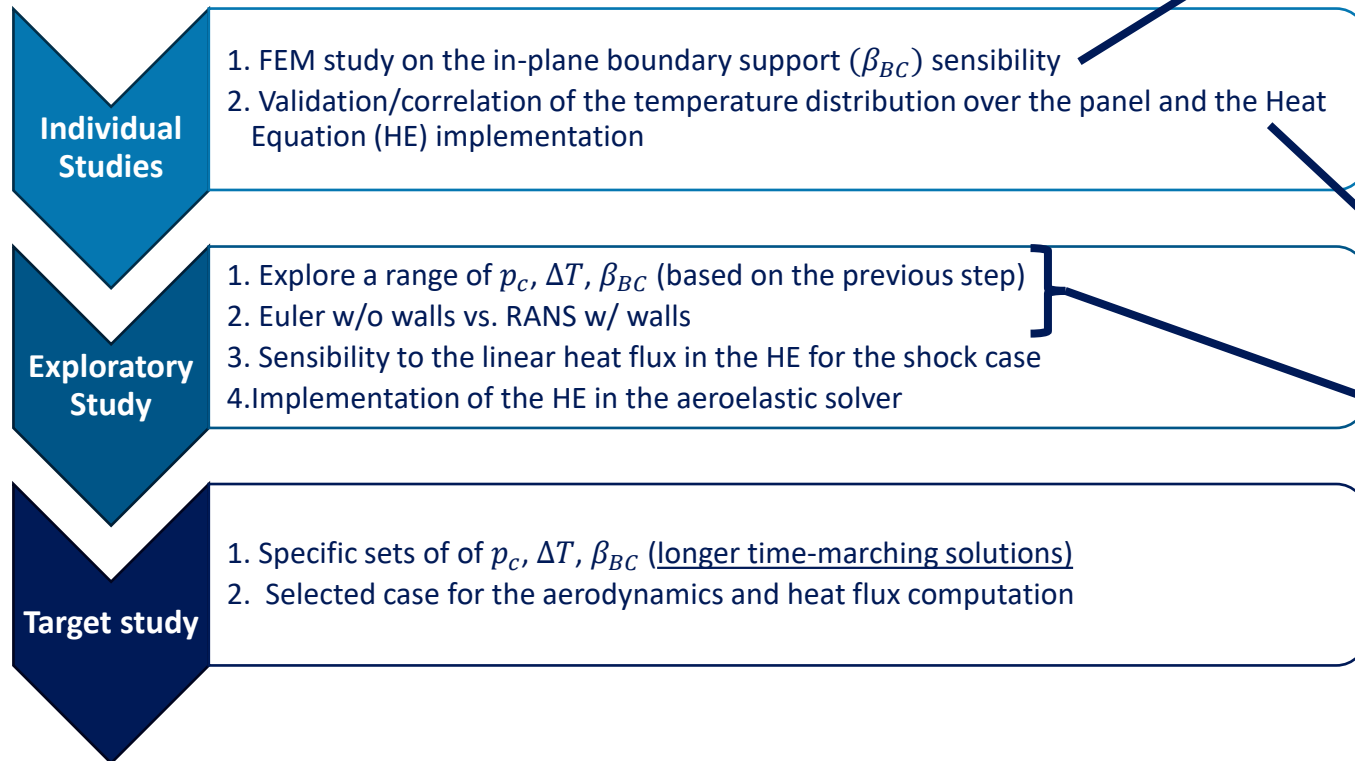


Fig. 2 Side view of plate, freestream flow, cavity, and in-plane edge stiffness  $K(x = [0,a], y)$ ; and cross section at  $-b/2 < y < +b/2$ .

Freydin and Dowell. AIAA(2020)

# Summary

- A range of aerodynamic models has been considered including piston theory, full potential flow, Euler flow and RANS with and without shock impingement.
- For the RC-19 configuration the **results are particularly sensitive to the pressure differential, thermal stress** (which leads to buckling) **and the in-plane as well as out of plane boundary support conditions** for the plate.
- A **finite element model** of the plate and its support structure allows the **determination of the effective in-plane support boundary condition**.
  - This information could also be obtained from an experiment to measure the change in natural frequencies due to a pressure differential.
- **Results for flutter and LCO** of the RC-19 experiment **are not particularly sensitive to the aerodynamic model**, with the key exception that the heating of the plate is due to the aerodynamic flow.
  - The thermal field needs to be determined by a RANS model or from experiment. Piston theory, potential flow theory and Euler flow all give similar results, but all require some auxiliary modeling of the heating due to the aerodynamic flow (e.g. Eckert model).
- Flutter and LCO results do become sensitive to  $M_\infty$  and other flow parameters in the low supersonic, transonic range and the results from the various aerodynamic models may vary substantially.



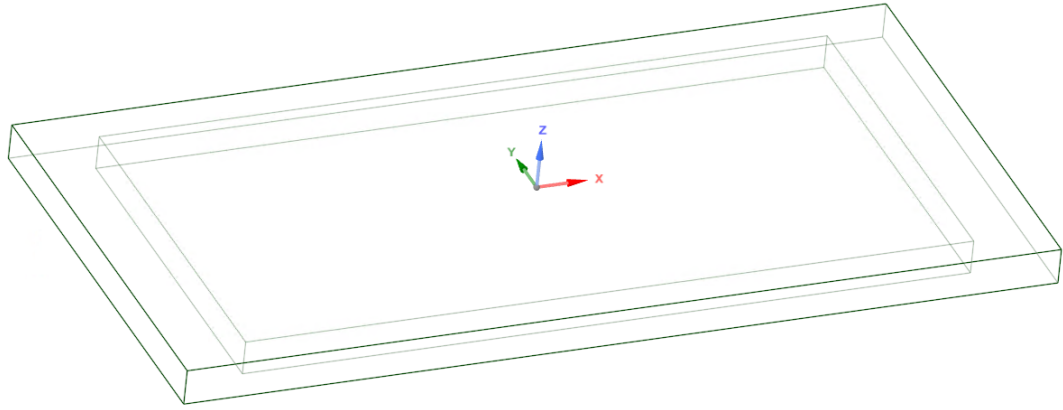
# Outline

- Computation of natural frequencies of a plate with changes in a  $\Delta p$  using a FEM of the plate and its support structure
  - This allows the determination of the effective in plane support spring stiffness for the plate.
- Correlation between the Heat Equation implementation and experimental data
- LCO correlation results
  - No-shock configuration (review from AePw3)
  - 4° shock wedge configuration using Euler and RANS models (preliminary results)

# FEM study on the $\beta_{BC}$ sensibility

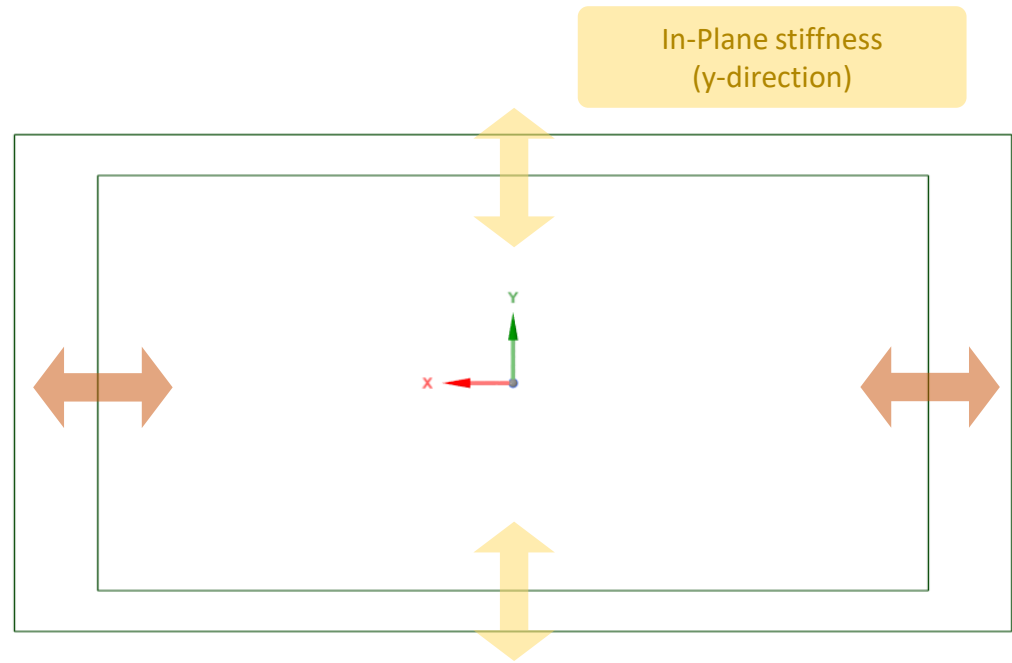
$$\beta_{BC} \equiv \frac{K_{BC}a}{Eh}$$

- Individual Studies
- Exploratory Study
- Target Study



0.305×0.152×0.0127 m block of AISI 4140 alloy steel with a machined pocket, leaving the thin panel (elastic structure)

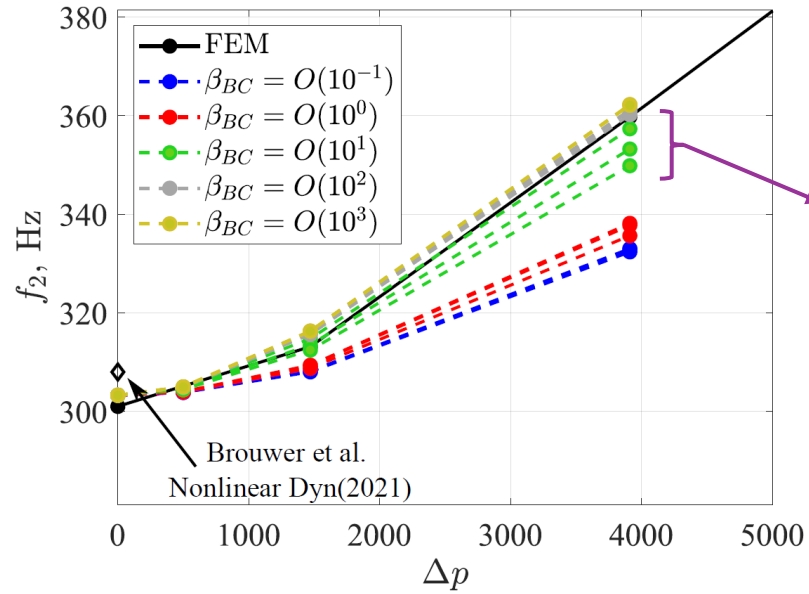
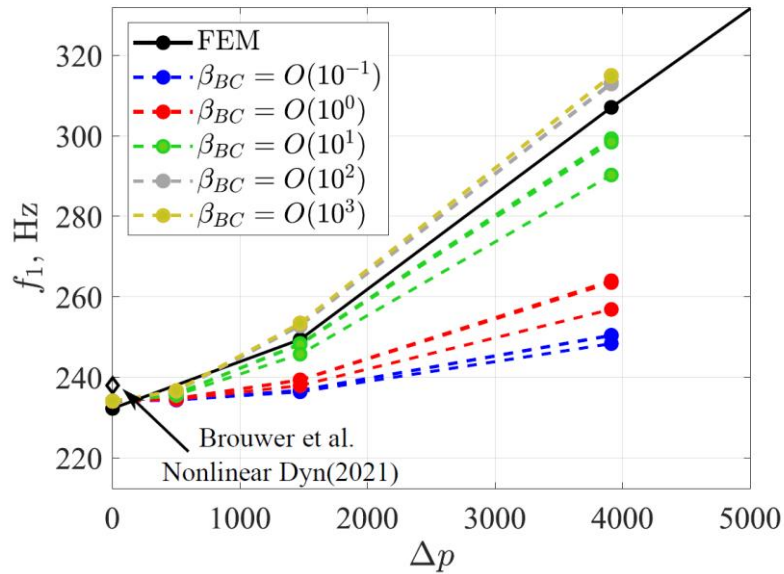
In-Plane stiffness (x-direction)



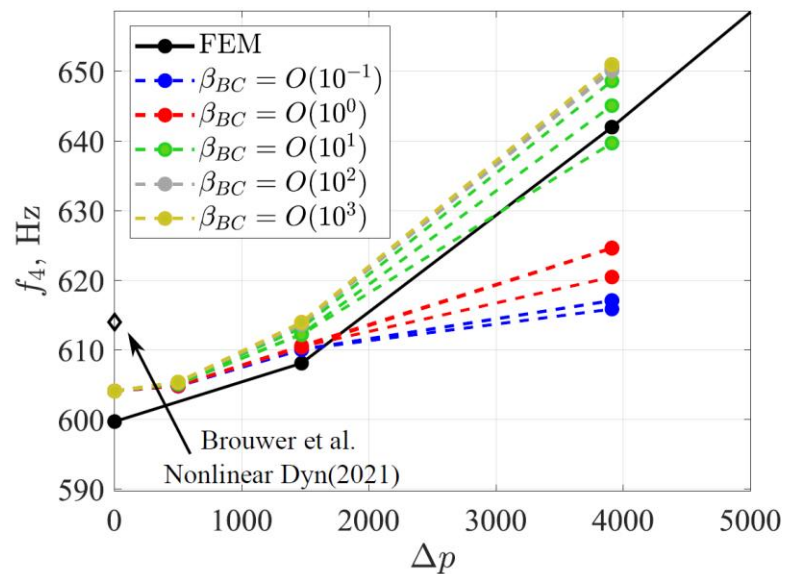
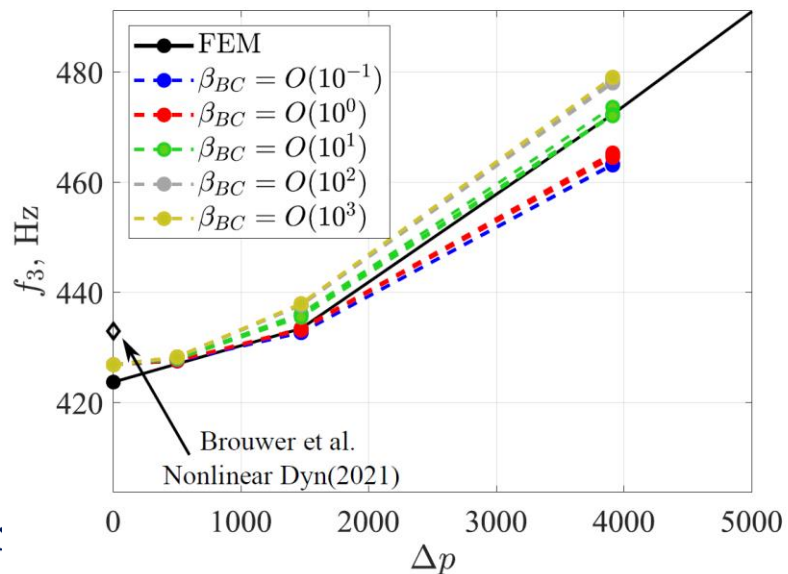
# $\Delta p$ vs. Natural Frequency: FEM vs. Aeroelastic Code

$$\Delta T = 0$$

$$U_\infty = 0$$



Plots include results for the symmetric ( $\beta_{BC,x} = \beta_{BC,y}$ ) and asymmetric ( $\beta_{BC,x} \neq \beta_{BC,y}$ ) in-plane stiffness, but they are roughly the same in all cases



Expected range for the RC-19 conf. :

$$O(10^1) < \beta_{BC} < O(10^2)$$



# Heat Equation (HE) Implementation

$$\underbrace{M_{m,n}\ddot{q}_n(t) + C_{m,n}\dot{q}_n(t) + G_{m,n}^{(1)}q_n(t)}_{\text{Linear plate model}} + \underbrace{D_{m,n,r,p}^{(2)}q_n(t)q_r(t)q_p(t)}_{\text{NL structural stiffness}} + \underbrace{G_{m,n,r}^{(3)}q_n(t)T_r(t)}_{\text{Thermal coupling}} + \underbrace{Q_{m,n}^{Aero} + Q_m^{static}}_{\text{Pressure terms}} = 0$$

$$\underbrace{M_{m,n}^H\dot{T}_n(t) + K_{m,n}^HT_n(t)}_{\text{Thermal inertia and stiffness}} + \underbrace{Q_m^0 + Q_{m,n}^q q_n(t) + Q_{m,n}^{\dot{q}}\dot{q}_n(t) + Q_{m,n}^{Tq}T_n(t)}_{\text{Coupled linear aerodynamic heating}} = 0$$

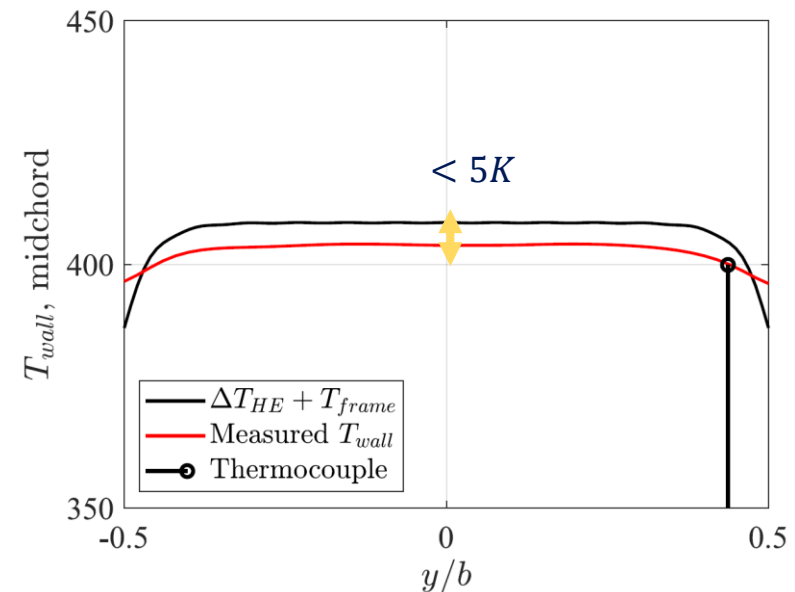
- The  $\Delta T$  measured by the thermocouple is slightly smaller than the mid-plate temperature
- The HE implementation overpredicts the mid-plate temperature by  $< 5K$



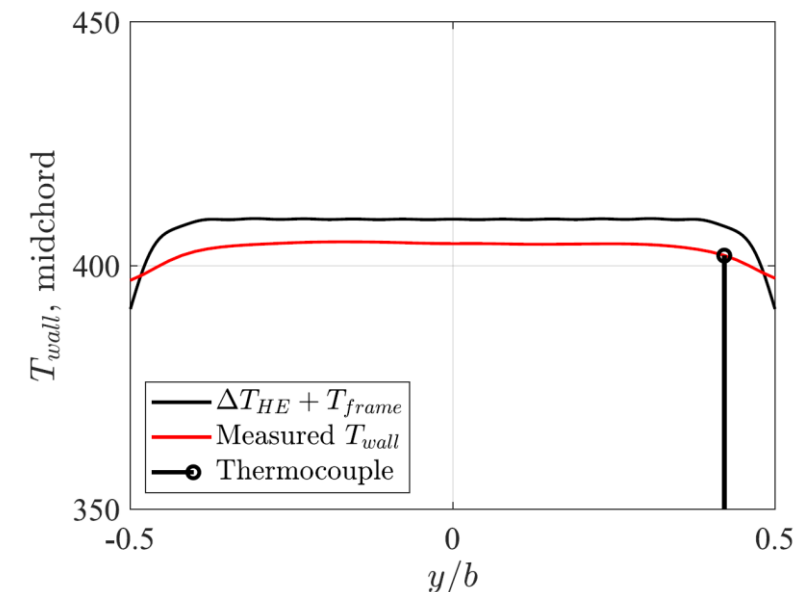
## Wind Tunnel Setup

Parameter	Value
$M_\infty$	1.92
$p_0$	$\approx 346$ kPa
$T_0$	$\approx 420$ K
$\Delta p$	0

## No shock



## 4° Wedge Shock



Different setup from the workshop case!



# Heat Equation (HE) Implementation

$$\underbrace{M_{m,n}\ddot{q}_n(t) + C_{m,n}\dot{q}_n(t) + G_{m,n}^{(1)}q_n(t)}_{\text{Linear plate model}} + \underbrace{D_{m,n,r,p}^{(2)}q_n(t)q_r(t)q_p(t)}_{\text{NL structural stiffness}} + \underbrace{G_{m,n,r}^{(3)}q_n(t)T_r(t)}_{\text{Thermal coupling}} + \underbrace{Q_{m,n}^{Aero} + Q_m^{static}}_{\text{Pressure terms}} = 0$$

$$\underbrace{M_{m,n}^H\dot{T}_n(t) + K_{m,n}^HT_n(t)}_{\text{Thermal inertia and stiffness}} + \underbrace{Q_m^0 + Q_{m,n}^q q_n(t) + Q_{m,n}^{\dot{q}}\dot{q}_n(t) + Q_{m,n}^{T_q}T_n(t)}_{\text{Coupled linear aerodynamic heating}} = 0$$

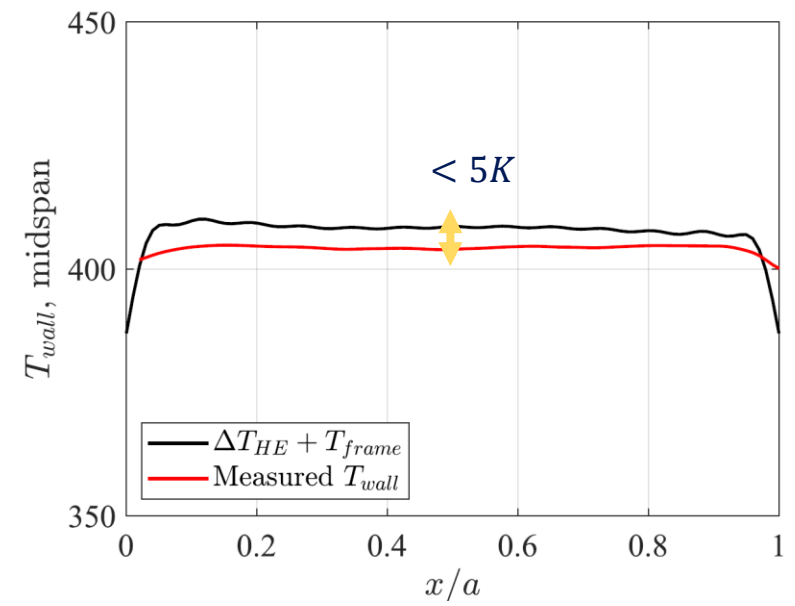
The HE implementation overpredicts the temperature at and after the shock location for the shock case (chord-wise)



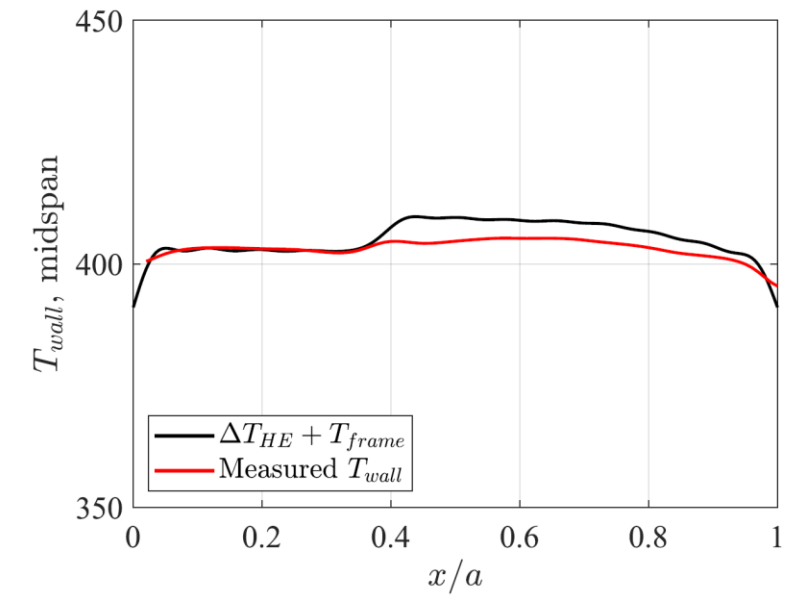
## Wind Tunnel Setup

Parameter	Value
$M_\infty$	1.92
$p_0$	$\approx 346$ kPa
$T_0$	$\approx 420$ K
$\Delta p$	0

## No shock



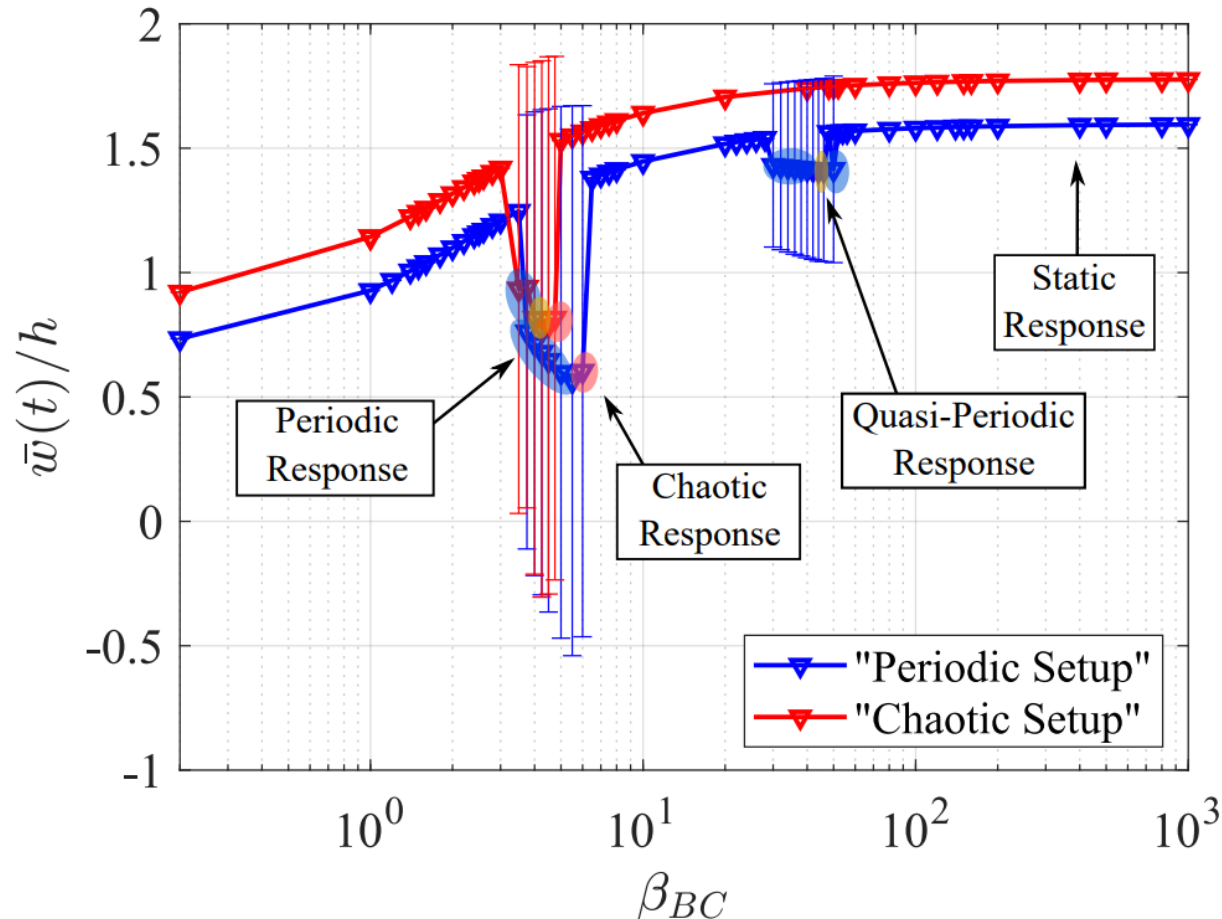
## 4° Wedge Shock



Different setup from the workshop case!

# Review from the AePW3: No-shock case

## Effect of In Plane Boundary Stiffness on Panel Response



	Periodic Parameters	Chaotic Parameters	
$\Delta p$ (kPa)	3.91	$\Delta p$ (kPa)	5.01
$\Delta T$ (K)	12.8	$\Delta T$ (K)	14.7

$\beta_{BC}$  can be determined from a ground vibration test of Finite Element Modeling of panel + its boundary support

$$\beta_{BC} \equiv \frac{K_{BC} a}{Eh}$$

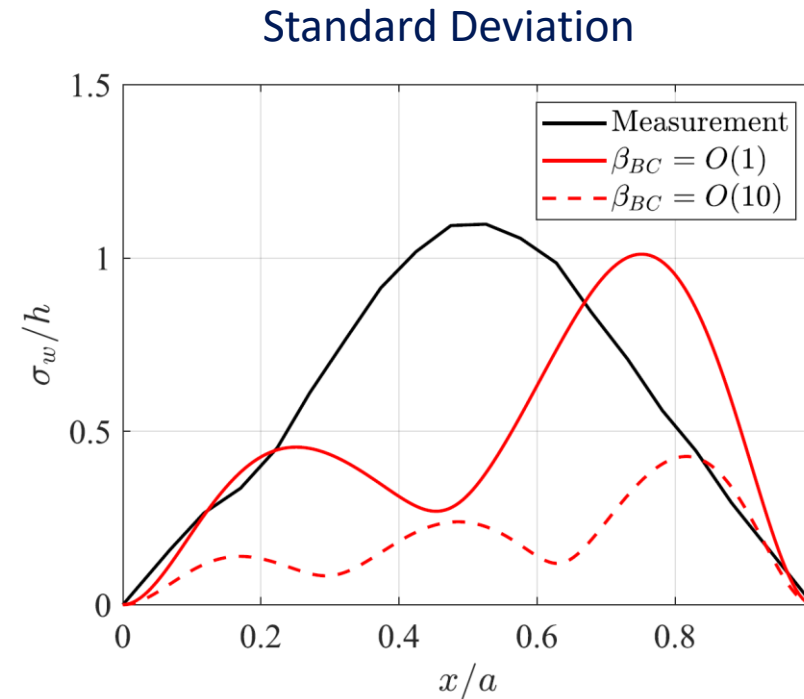
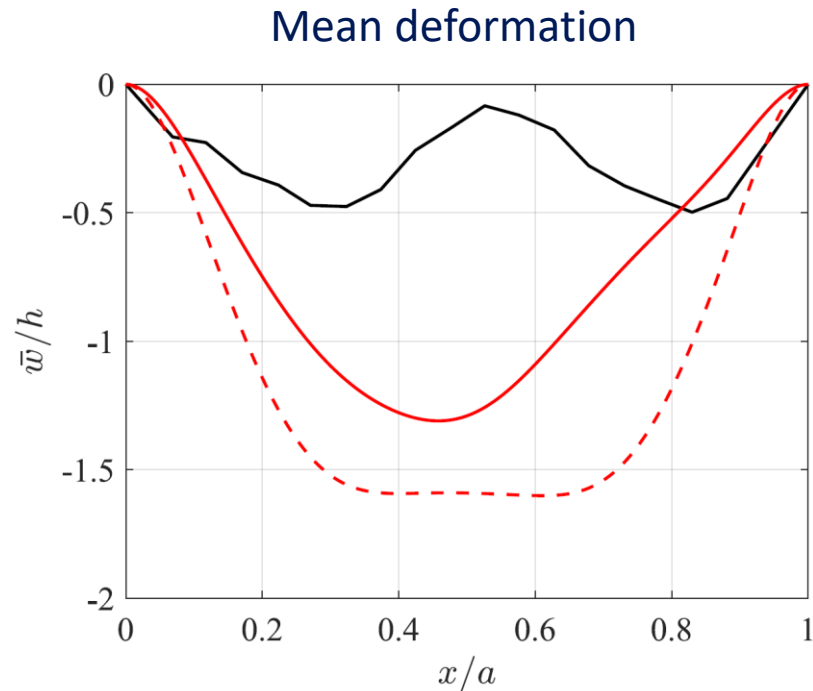
# Correlation with Measurement: “Periodic” LCO

## Periodic Parameters

$\Delta p$  (kPa) 3.91

$\Delta T$  (K) 12.8

**Aerodynamic Model:** Piston Theory,  $M_\infty = 1.94$ , no wind tunnel walls



Bigger  $\beta_{BC}$  leads to bigger static deformation, and smaller LCO amplitude

The enforced  $\Delta p$  is the main reason for the big difference in the mean deformation between experiment and computational results



# Correlation with Measurement : “Chaotic” LCO

## Chaotic Parameters

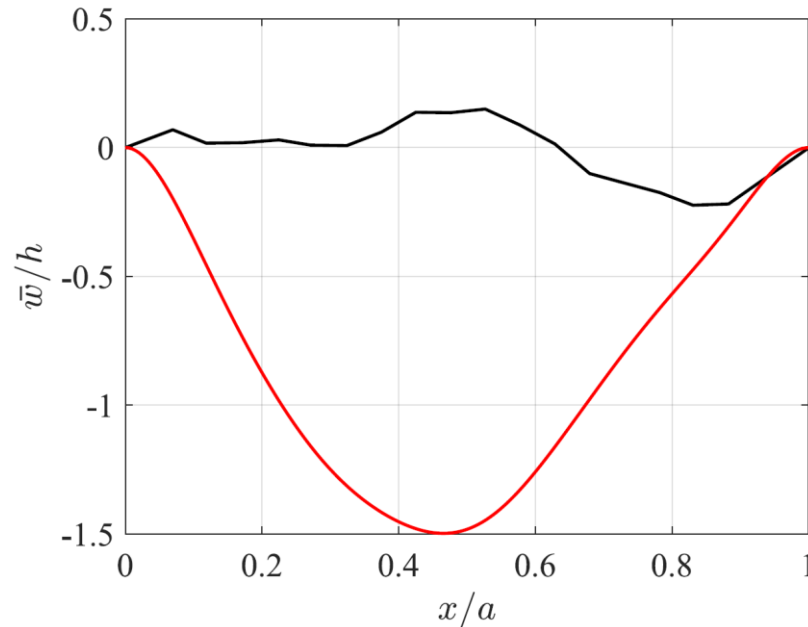
$\Delta p$  (kPa) 5.01

$\Delta T$  (K) 14.7

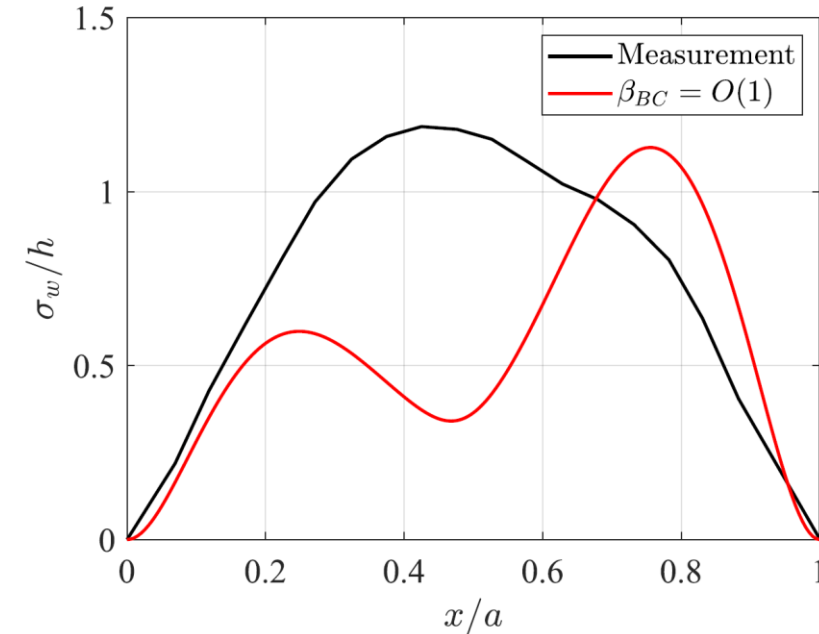
**Aerodynamic Model:** Piston Theory,  $M_\infty = 1.94$ , no wind tunnel walls



Mean deformation



Standard Deviation

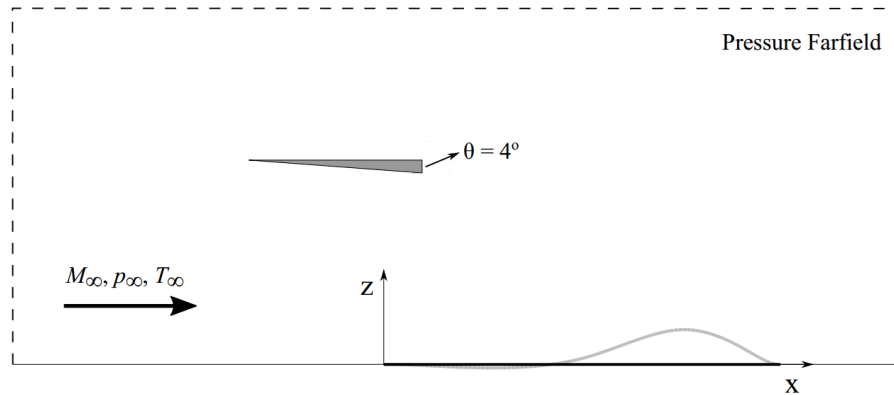


LCO was only found for  $\beta_{BC} = O(1)$

Again, the enforced  $\Delta p$  is the main reason for the big difference in the mean deformation between experiment and computational results

# Shock Impingement Case: Correlation with experimental data

## Preliminary Results



**Aerodynamic Model:**  
Euler/DLTA  
 (Dynamically Linearized Time-Domain Approach)

### ~~Wind Tunnel walls~~

In-Plane boundary stiffness

$M_\infty = 2.0$  on the wall

$\Delta T$  between panel and frame

$\Delta p$  between fluid and acoustic cavity

Individual Studies

Exploratory Study

Target Study

**Aerodynamic Model:**  
RANS/DLTA  
 (Dynamically Linearized Time-Domain Approach)

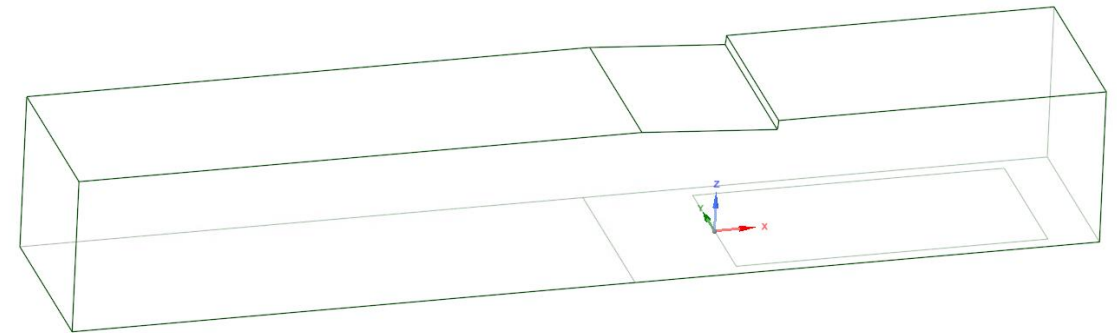
### Wind Tunnel walls

In-Plane boundary stiffness

$M_\infty = 1.92$  on the wall

$\Delta T$  between panel and frame

$\Delta p$  between fluid and acoustic cavity



SST  $k - \omega$   
 $y^+ = 5$

$\delta_{LE} \approx 8\text{mm}$  (Wind Tunnel:  $\delta_{LE} \approx 8.6\text{mm}$ )  
 $\delta_{LE}/a \approx 0.03$  (Wind Tunnel:  $\delta_{LE}/a \approx 0.033$ )

# Aeroelastic solution for a range of $p_c$ , $\Delta T$ , and $\beta_{BC}$

## Exploratory parameters

$\beta_{BC} = [0.1, 1000]$   $\rightarrow$  we're computing the solution at this stage for a wider range of in-plane stiffness, although we have an "expected range" for this parameter predicted by the FEM study.

$\Delta T = 15 \text{ K}$   $\rightarrow$  considers the small increase in temperature between the thermocouple location ( $\Delta T = 13.3 \text{ K}$ ) and the mid-plate

$\Delta T = 20 \text{ K}$   $\rightarrow$  considers the overshoot from the HE solution

Uniform Distribution for  $\Delta T$

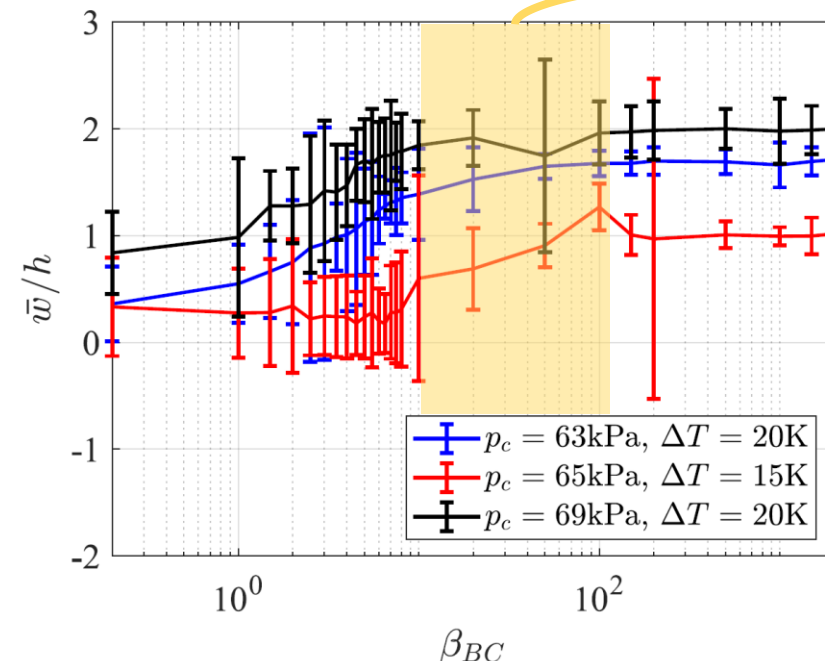
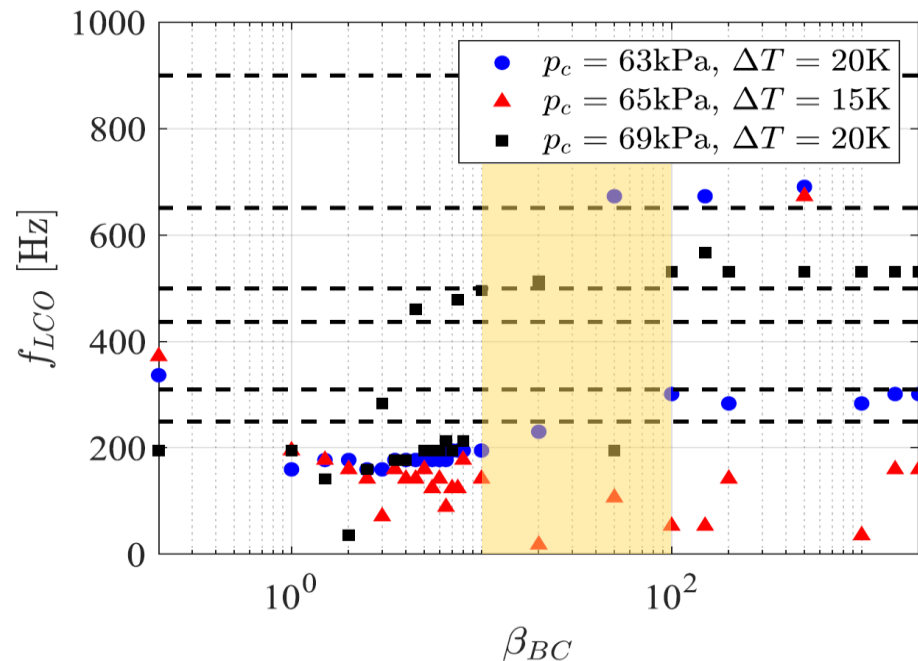
$p_c = 69 \text{ kPa}$   $\rightarrow$  the same as the wind tunnel setup

$p_c = 63$  and  $65 \text{ kPa}$   $\rightarrow$  considers a smaller cavity pressure to assess the LCO behavior after the shock location

Individual Studies

Exploratory Study

Target Study



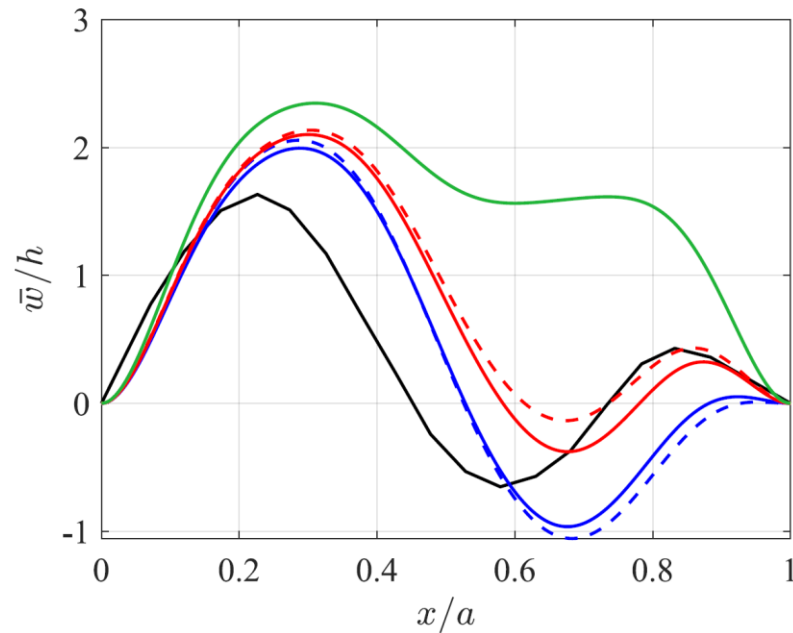
$\beta_{BC}$  range from the FEM study

# Aeroelastic solution for a range of $p_c$ , $\Delta T$ , and $\beta_{BC}$

Aerodynamic Model: Euler/DLTA,  $M_\infty = 2.0$ , no wind tunnel walls



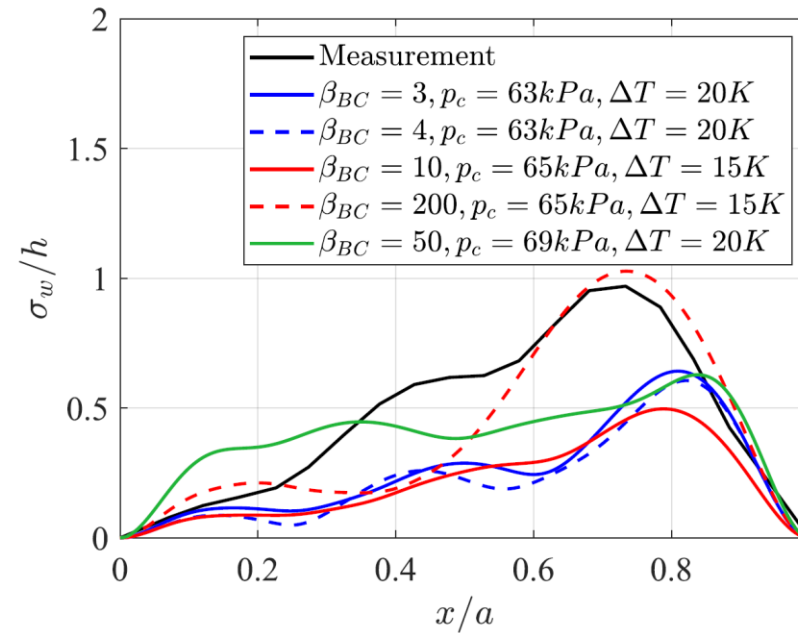
Mean deformation



Bigger  $\Delta T$  leads to bigger mean deformation in the post shock region

$p_c = 69$  kPa keeps all oscillations above the y-axis line

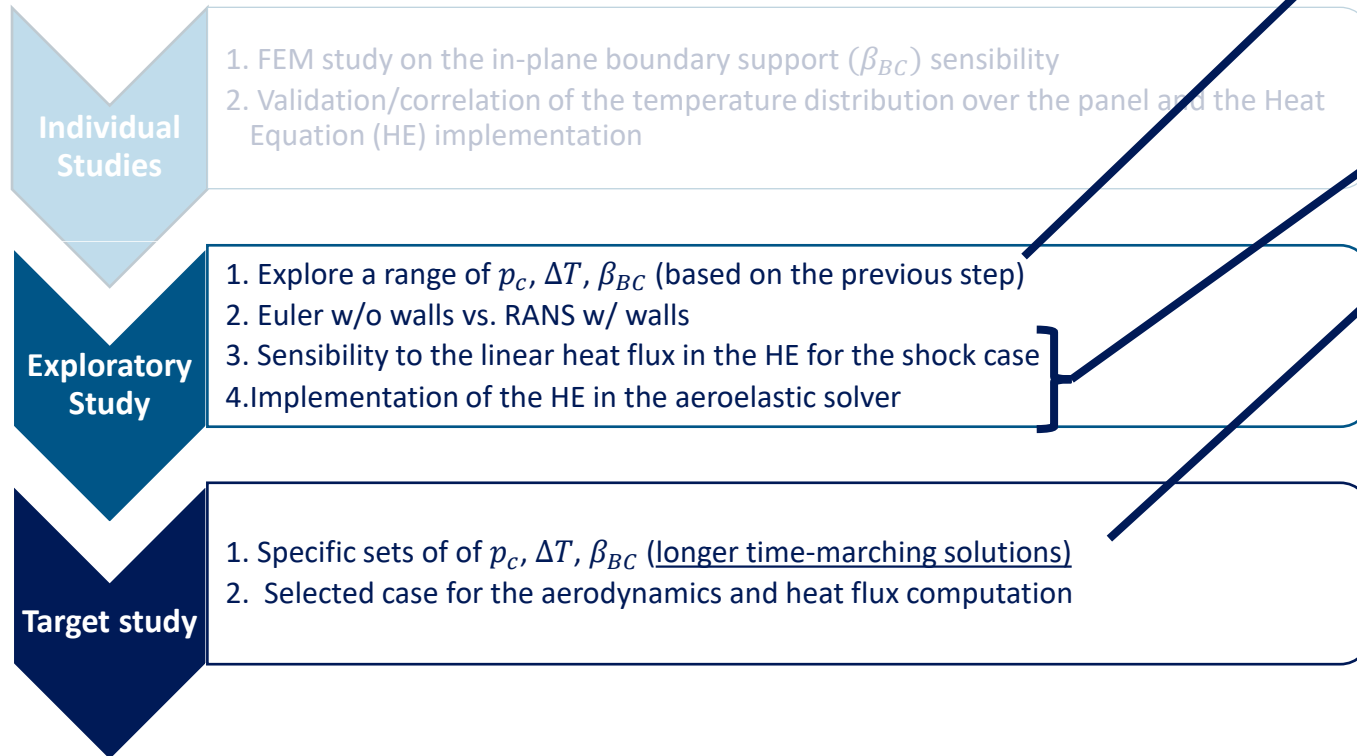
Standard Deviation



LCO after the shock location more sensitive to the smaller  $\Delta T$  conf.

$p_c = 69$  kPa leads to a "first mode-shape" deformation

Very chaotic LCO



## Next Steps

- Implement the DLTA (Euler or RANS) to the no-shock configuration and correlate with measurements
- Implement the aeroelastic solver coupled with the Heat Equation.
- “Target study”

Additional step:

$8^\circ$  shock wedge configuration: assess the modal convergence and the (potential) fluid instability after the wedge body



# AePW-3

# High Speed Working Group

## RC-19 Wind Tunnel

2024 Updates

Aeroelasticity Laboratory | Duke University

Luisa Piccolo Serafim, Earl Dowell